

Modeling the therapeutic pharmacokinetics of AMG 181, a monoclonal antibody against a4b7 in humans, for the treatment of inflammatory bowel disorders

¹DR C. RENUKATEJASWINI,²R. JONA METHUSULA,³ DR R SRIRAM,
⁴E. HONEY,⁵R. NAGANJANEYULU

Department of Pharmacology, Dr K.V Subba Reddy Institute of Pharmacy

Abstract

Using pharmacokinetic (PK) and pharmacodynamic (PD) data from cynomolgus monkeys, this research aimed to estimate a safe starting dosage of AMG 181, a human anti-a4b7 antibody for treating inflammatory bowel disorders. The AMG 181 PK in cynomolgus monkey was studied using a two-compartment model that included target-mediated drug disposition in addition to parallel linear drug distribution. In order to forecast PK in humans, the calculated parameters were allometrically scaled. Data on the relationship between AMG 181 concentration and free a b receptor in cynomolgus monkeys was analyzed using an Emax PD model. The clinical dosages of AMG 181 were chosen after considering the levels of exposure in monkeys at which no adverse effects were detected (80 mg·kg⁻¹), the levels likely to be experienced by humans, and the concentration of AMG 181 that is expected to result in higher than 50% occupancy of the a4b7 receptor in humans. The central volume of distribution was 2900 mL and the estimated clearance for AMG 181 in humans was 144 mL·day⁻¹. One 14 ng·mL⁻¹ EC₅₀ was calculated for the free a4b7 receptor. When faced with

Humans were projected to have exposure margins over 490,000 at a starting dosage of 0.7 mg, while AMG 181 concentrations were projected to only momentarily cover the free a4b7 receptor EC₁₀. Between 7 mg subcutaneous and 420 mg intravenous, the predicted C_{max} and AUC were consistent with the first-in-human trial. For human AMG 181 testing, the created model was useful in deciding on a safe initial dosage and a method for pharmacologically appropriate dose escalation. The model developed using data from cynomolgus monkeys was shown to be accurate by the clinically observed human AMG 181 PK.

Abbreviations

AUC, area under the concentration–time curve; CD, Crohn’s disease or cluster of differentiation; CHO, Chinese Hamster Ovary cells; CL, Clearance; C_{max}, maximum observed concentration; EC₅₀, concentration at half-maximal effect; ECL, electro- chemiluminescence; F₁, subcutaneous bioavailability; GLP, good laboratory practice; HEK, human embryonic kidney cells; IBD, inflammatory bowel diseases; IgG, immunoglobulin G; IIV, interindividual variability; IV, intravenous(ly); JC virus, John Cunningham polyomavirus; K_A, absorption rate constant; K_D, dissociation constant; K_{int}, internalization rate constant; K_m, Michaelis–Menten constant; K_{ss}, quasi-steady-state constant; LLOQ, lower limit of quantification; MAdCAM-

Introduction

mucosal addressin cell adhesion molecule 1; M-M, Michaelis–Menten; NIH, National Institutes of Health; PBMC, peripheral blood mononuclear cells; PD, pharmacodynamics(s); PK, pharmacokinetic(s); PML, progressive multifocal leukoencephalopathy; QE, quasi-equilibrium; QSS, quasi-steady state; R_{tot}, total receptor concentration; SC, subcutaneous(ly); TMDD, target-mediated drug disposition; UC, ulcerative colitis; V_c, central volume of distribution; V_{max}, maximum nonlinear elimination rate; VPC, visual predictive check.

Crohn’s disease (CD) and ulcerative colitis (UC) are the

two major types of inflammatory bowel diseases (IBD). Currently, anti-tumor necrosis factor agents (anti-TNFs) are the main class of approved biologics for treating CD and UC. However, there is a need for development of new therapeutics for those patients who do not respond or have developed tolerance to anti-TNFs after initial treatment. Therapies that block the influx of pro-inflammatory cells into the intestinal mucosa through integrin-mediated leukocyte tethering, rolling, and arrest (Hynes 2002) have gained attention in recent years.

Preclinical animal models have demonstrated the roles and benefits of blocking lymphocyte intestinal homing through antagonism of integrin *a4b7* (Hesterberg et al. 1996; Fedyk et al. 2012; Pan et al. 2012), integrin *b7*

(Wagner et al. 1996; Apostolaki et al. 2008; Stefanich et al. 2011), and integrin $\alpha_4\beta_7$ ligand MAdCAM-1 (Picarella et al. 1997; Pullen et al. 2009). There are currently several IBD treatments targeting leukocyte migration and adhesion in clinical development, including vedolizumab (anti- $\alpha_4\beta_7$), etrolizumab (anti- β_7), PF-00547659 (anti-MAdCAM-1), GSK-1605786 (anti-CCR9), and AJM300

(anti- α_4) (Thomas and Baumgart 2012; Lobaton et al. 2014). Natalizumab (anti- α_4) has been approved in the United States for the treatment of CD (Sandborn et al. 2005; Targan et al. 2007) and vedolizumab has shown clinical benefits in treating both CD and UC (Feagan et al. 2005, 2008; Parikh et al. 2011).

Natalizumab is a humanized immunoglobulin (Ig) G₄ antibody targeting α_4 and is thus antagonistic against both $\alpha_4\beta_1$ for treating relapsing and remitting forms of multiple sclerosis (Polman et al. 2006) and $\alpha_4\beta_7$ for treating CD (Sandborn et al. 2005). Natalizumab-mediated inhibition of trafficking of $\alpha_4\beta_1$ -expressing leukocyte to the central nervous system through pan- α_4 inhibition may be linked to progressive multifocal leukoencephalopathy (PML) caused by reactivation of latent human John Cunningham (JC) polyomavirus infection (Berger and Koralknik 2005). Additionally, natalizumab as well as vedolizumab (IgG₁) are humanized antibodies and have shown greater than 10% immunogenicity in IBD patients leading to diminishing clinical efficacy (Feagan et al. 2005, 2008; Sandborn et al. 2005; Parikh et al. 2011). To reduce or eliminate the immunogenic response and also avoids targeting the $\alpha_4\beta_1$ -expressing leukocytes implicated in the occurrence of PML reported previously in natalizumab-treated patients. Comprehensive investigational results from AMG 181 in vitro pharmacology experiments and in vivo pharmacokinetic and toxicology studies have been published previously (Pan et al. 2013).

Several recent publications have summarized methods for the first-in-human (FIH) dose estimation (Gibbs 2010; Chen et al. 2012; Zou et al. 2012). Here, a quantitative translation of AMG 181 in vitro and in vivo pharmacology from cynomolgus monkeys to humans is presented that uses 70% and 90% levels of $\alpha_4\beta_7$ receptor occupancy to guide the selection of a safe starting dose and pharmacologically relevant single and multiple dose escalation schemes for Phase 1 clinical trials in healthy volunteers and IBD subjects (www.clinicaltrials.gov, study identifiers NCT01164904 and NCT01290042). Comparison with the clinical PK from the single-dose Phase 1 study (Pan et al. 2014) validated our modeling predictions.

Materials and Methods

In vitro pharmacology studies

AMG 181 (~144 kD) was manufactured at Amgen Inc. (Thousand Oaks, CA) by expression in a Chinese hamster ovary (CHO) cell line (Hsu et al. 2010). Results from in vitro pharmacology studies including $\alpha_4\beta_7$ target receptor occupancy on CD4⁺ T-cell subsets, including central memory, effector memory, and naïve

T, have been reported previously (Pan et al. 2013).

In vivo studies in cynomolgus monkeys

Male and female cynomolgus monkeys (*Macaca fascicularis*), ranging from 2.1 to 6.4 kg, were cared for in accordance with the Guide for the Care and Use of Laboratory Animals, 8th Edition (National Research Council US 2011). Animals were socially housed at an indoor, AAALAC, Intl-accredited facility in species-specific housing. All research protocols were approved by the Institutional Animal Care and Use Committee. Animals were

fed a certified pelleted primate diet (PMI #5048, Richmond, IN) daily in amounts appropriate for the age and size of the animals, and had ad libitum access to water (municipality tap water processed through a reverse osmosis filter and passed through ultraviolet light treatment) via automatic watering system/water bottle. Animals were maintained on a 12:12 h light:dark cycle in rooms at 18–29°C (30–70% humidity) and had access to enrichment opportunities (small bits of fruit, cereal, or other treats). All animals were negative for simian retrovirus.

Cynomolgus monkeys were assigned to treatment groups for two single-dose PK/PD Studies A and C, a two-dose (2-weekly doses) toxicology Study B, a 3-month (13-weekly doses; Study D), and a 6-month (24-weekly doses; Study E) Good Laboratory Practice (GLP) toxicology study (Table 1). Pre- and postdose blood samples were collected for PK/PD and immunogenicity assessments. Postdose observations in toxicology studies were conducted to assess the safety of AMG 181. PK samples from the PK/PD studies and the non-GLP toxicology study were analyzed for AMG 181 using an electrochemiluminescence (ECL) immunoassay with a lower limit of quantification (LLOQ) of 2 ng·mL⁻¹. The GLP toxicology study used an ECL immunoassay with a LLOQ of 20 ng·mL⁻¹.

Serum samples were analyzed for anti-AMG 181-specific antibodies (antidrug antibodies; ADAs) using a validated immunoassay with a lower limit of reliable detection (LLRD) of 20 ng·mL⁻¹ rabbit anti-AMG 181 polyclonal antibody in neat pooled cynomolgus monkey serum. Samples with values greater than the predefined assay-specific cut point ranging from 1.08 to 1.14 based on the signal-to-noise ratio (fold difference in the anti-AMG 181-specific antibodies assay signal of samples or positive controls relative to the assay background assessed by the negative control) were defined as ADA positive.

AMG 181 PK data for modeling

PK data were collected from a total of 119 monkeys (73 males and 46 females) actively treated with AMG 181 for up to 420 days after the first dose, with 86 receiving SC and 33 receiving IV dose(s). The median body weight of the monkeys was 2.8 kg (mean: 3.43 kg; range: 2.1–6.4 kg). In all five studies, anti-AMG 181 antibodies or immunogenic response was observed in a majority of the monkeys, except for those dosed 80 mg·kg⁻¹ SC or IV. In many cases, the presence of anti-AMG 181 antibodies clearly impacted the PK. Data

point exclusion was based on a two-step process: In a first step, candidates for exclusion were identified based on ADA positivity. In the second step, only data points where PK was also visually impacted were excluded (Fig. S2). This approach resulted in removal of 120 out

of the 1743 (6.88%) available PK data points. The remaining 1623 AMG 181 concentration–time values were used for compartmental PK modeling.

model comparison on file). For the high multiple doses of 20–80 mg·kg^{−1}, which are especially relevant for prediction of clinically relevant doses, the M-M model did not predict the terminal phase as well as the TMDD model. The TMDD model parameters included: the first-order SC absorption rate constant (K_A), central volume of distribution (V_c), linear clearance (CL), the distribution rate constants between the central and peripheral compartments K_{12} and K_{21} , the total a_4b_7 receptor concentration (R_{tot}), the internalization rate constant of drug–receptor complex (K_{int}), and the QSS constant $K_{ss} = (k_{int} + k_{off})/k_{on}$, or the dissociation constant $K_d = k_{off}/k_{on}$ for QE model (Fig. 1). TMDD QSS/QE modeling was conducted on molar transformed AMG 181 concentration data with the free AMG 181 concentration (C_f) calculated using the equation shown in Figure 1. The K_d was fixed at 0.013 nmol/L, the EC₅₀ value of AMG 181 binding to monkey primary T cells in vi- tro.

drug disposition (TMDD) and quasi-equilibrium (QE) approximation.

PK variability models

Values for interindividual variability (IIV) of K_A , CL, V_c , and R_{tot} were estimated assuming lognormal distribution. The residual variability was assumed to have a mixture of proportional plus additive distribution.

Estimation method, diagnosis, and validation

PK datasets and results were constructed, tabulated, and plotted using S-PLUS® (Version 8.2, November 2010; TIBCO Software Inc., Palo Alto, CA) or SigmaPlot (Version 12.5; Systat Software, Inc., Chicago, IL, USA). Modeling of the monkey PK data and simulation of the human PK profiles were performed using nonlinear mixed-effects modeling using NONMEM®, Version 7.2 with gfortran FORTRAN compiler (Beal et al. 2009).

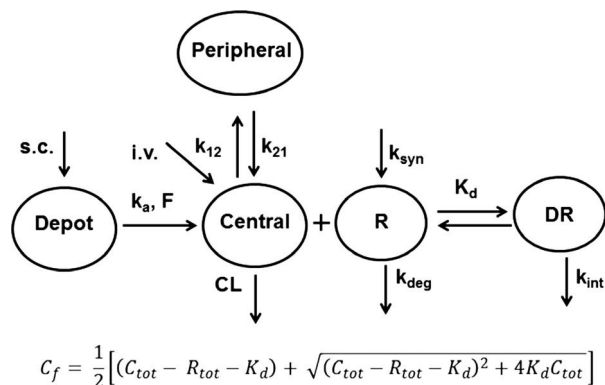


Figure 1. Schema of the two-compartment PK model with target-mediated

The first-order conditional estimation method with interaction (FOCE INTERACTION) was used to estimate the population PK parameters. Importance sampling method, with EONLY = 1 (“evaluation only”), was applied to facilitate obtaining the standard error of model parameters.

Model selection was guided by visual inspection of goodness-of-fit plots, parameter estimate precision/plausibility, and comparison of objective function values. All parameter estimates were reported with the relative standard error of the estimates (%SE). Internal model validation was carried out by visual predictive check (VPC) plots; four hundred datasets were simulated based on final parameter estimates and the estimated 10th, 50th, and 90th percentiles of the simulated AMG 181 concentration–time profiles were plotted against the observed data.

AMG 181 PD data and modeling

Study A was a dedicated PK/PD study in cynomolgus monkeys, where AMG 181 occupancy of free a_4b_7 on CD4+ T cell and its subsets were evaluated ex vivo. Mean fluorescence intensity (MFI) readings of free a_4b_7 and the time-matched AMG 181 concentrations in serum were used for curve fitting using an E_{\max} model:

$$E = E_o(1 - E_{\max}C/(EC_{50} + C)),$$

where the effect (E or MFI) was estimated through baseline (E_o), maximum effect (E_{\max}), AMG 181 concentration at half-maximal effect (EC_{50}), and AMG 181 concentration (C). Subsequent calculations for EC_{75} , EC_{90} , and EC_{99} and the AMG 181 concentrations at 75%, 90%, and 99% maximal effect, respectively, were carried out based on the E_{\max} model. Results from Studies B–E were not used for PD modeling due to high data variability and limited availability (especially GLP studies).

Allometric scaling and simulation of human PK

For the prediction and simulation of human PK, the structural PK models developed for cynomolgus monkeys (median observed body weight of 2.8 kg) were assumed to also describe AMG 181 disposition in humans (assumed median body weight of 70 kg) with parameters allometrically scaled (Dong et al. 2011). The AMG 181 CL and V_c values in human were determined from those in cynomolgus monkey by scaling by body weight ratio with exponents of 0.75 and 1, respectively. The distribution rate constants (K_{12} and K_{21}) were scaled with an exponent of -0.25 . The K_d constant was fixed at 0.031 nmol/L, the EC_{50} value of AMG 181 in vitro

binding potencies to human primary T cells. Other PK parameters including K_A , F_1 , R_{tot} , and K_{int} were assumed to be equivalent for cynomolgus monkeys and humans.

Exposure margins and FIH dose selection

The exposure margins were calculated based on the observed AMG 181 C_{max} ($4850 \text{ } \mu\text{g}\cdot\text{mL}^{-1}$) and area under the concentration–time curve (AUC, $485,000 \text{ h}\cdot\mu\text{g}\cdot\text{mL}^{-1}$) values in cynomolgus monkeys at the no observed adverse effect level (NOAEL; Study D) of $80 \text{ mg}\cdot\text{kg}^{-1}$ IV divided by the predicted human C_{max} and AUC values.

AMG 181 doses for the FIH study were selected based on: the exposure margins; the duration of serum AMG 181 concentration above 50–90% a_4b_7 receptor occupancy; and the maximum recommended starting dose (MRSD) in humans according to the United States Food and Drug Administration (US FDA) guidance (FDA 2005).

Comparison of predicted versus observed AMG 181 PK in humans

The predicted AMG 181 AUC and C_{max} in humans were compared to the AMG 181 PK parameters observed in the FIH study with doses ranging from 7 mg SC to 420 mg IV. Data from the FIH study of AMG 181 have been reported separately (Pan et al. 2014).

Results

Compartmental modeling of AMG 181 PK in cynomolgus monkeys

In the final model, the individual AMG 181 concentration–time data for all cynomolgus monkeys from Studies A–E were simultaneously fit using a two-compartment TMDD QE PK model (Fig. 1). This model performed well for single and multiple dose administration with the exception of lowest single-dose cohort ($0.01 \text{ mg}\cdot\text{kg}^{-1}$ IV), where the model underpredicted the observed concentrations (Fig. 2). The diagnostic plots presented in Figure 3 suggest that the PK model characterized the observed concentration–time data well. Some divergence from the line of identity was observed at higher concentrations in the DV versus PRED plot. This deviation may have been due, in part, to the attempt to reconcile the PK from the $80 \text{ mg}\cdot\text{kg}^{-1}$ IV and SC doses, where SC dosing resulted in higher exposure compared to the IV dose (Fig. S1A).

Table 2 summarizes the AMG 181 population parameters and IIV in cynomolgus monkeys estimated in the final model. The population PK parameter estimates as well as the IIVs were generally well estimated with relative

standard error (%SE) of less than 30%. In Studies A, C, and D, where AMG 181 was administered both SC and IV, relative bioavailability after SC was estimated to be 80–96% via noncompartmental analysis. In our first PK modeling attempt, the SC bioavailability (F_1) was initially estimated to be close to 1 and was subsequently set to 1.0 (or 100%) to stabilize the model and to provide a conservative approach when the same assumption was also applied in prediction of human PK. No IIV on F_1 was estimated.

The estimated population central volume of distribution (V_c) was 116 mL, which is physiologically plausible for a typical 2.8 kg cynomolgus monkey (Davies and Morris 1993). Based on the typical PK parameters, the linear elimination half-life of AMG 181 was estimated to be 12 days. Since the target (a_4b_7 receptor) concentrations were not available and few drug concentrations were measured at the terminal phase, R_{tot} and K_d could not be simultaneously estimated. Therefore, K_d was fixed to 0.013 nmol/L , the EC_{50} value of AMG 181 binding to a_4b_7 receptors on monkey primary T cells in vitro, in the final model and R_{tot} was estimated relative to this assumption (Table 2).

Figure 4 shows the internal model validation carried out using visual predictive checks (VPC). With 400 datasets simulated based on final parameter estimates, the estimated medians and the two-sided 80% prediction intervals (10th, 50th, and 90th percentiles) of the simulated AMG 181 concentration–time profiles contained the observed PK data well, especially in light of the small sample sizes per dose group and over an 8000-fold dose range (0.01 – $80 \text{ mg}\cdot\text{kg}^{-1}$).

Modeling of AMG 181 PD in cynomolgus monkeys

For Study A, individual observed free a_4b_7 receptor on total $CD4^+$ T cells (measured as MFI) versus AMG 181 concentration data is compared to the model fit in Figure 5. The estimated PD model parameters were 531 (MFI), 0.922, and $0.0140 \text{ } \mu\text{g}\cdot\text{mL}^{-1}$ for E_0 , E_{max} , and EC_{50} , respectively. Based on the model, the calculated values for EC_{75} , EC_{90} , and EC_{99} are 0.042, 0.126, and $1.38 \text{ } \mu\text{g}\cdot\text{mL}^{-1}$, respectively.

As a pharmacologic consequence of a_4b_7 occupancy, counts of total $CD4^+$ T cell and its subsets, including naïve and central memory cell counts, were elevated due to the inhibition of their trafficking into the intestinal tissues. Because the $CD4^+$ T cell and its subset count data were sparse and highly variable in all studies, PD modeling attempts using cell count measures were not successful: qualitative assessments have been reported elsewhere (Pan et al. 2013).

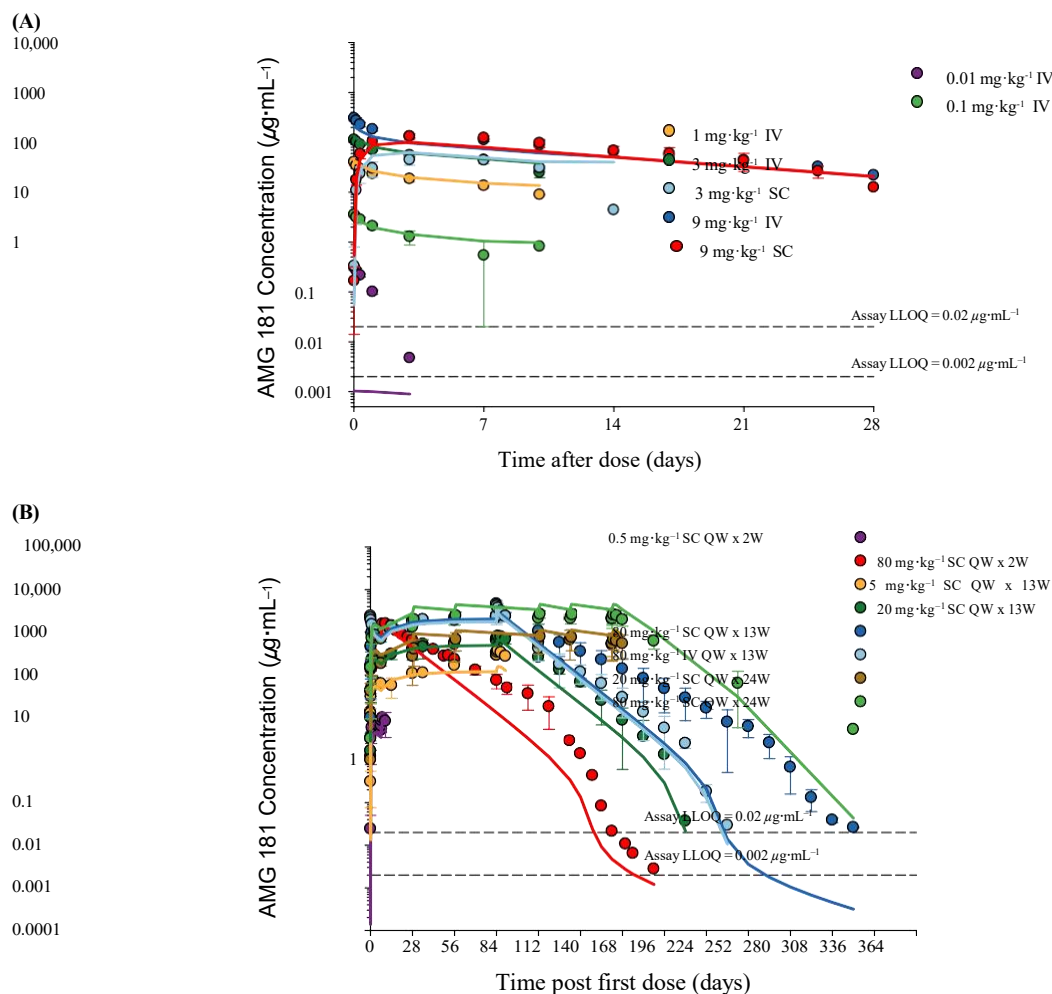


Figure 2. Simultaneous fitting of the individual AMG 181 concentration–time data from all cynomolgus monkeys using the two-compartment TMDD QE PK model: (A) Single IV or SC dose and (B) 2-weekly, 13-weekly, or 24-weekly IV or SC doses. Symbols represent mean (SD) observations. Solid lines represent the mean of model predicted individual concentration–time profiles in the respective cohort.

Allometric scaling, simulation, and dose selection in humans

The estimated AMG 181 PK parameters in humans, determined through allometric scaling from parameters determined in cynomolgus monkeys, are presented in Table 3. These PK parameters (e.g., CL and V_c) are physiologically reasonable for kinetics of monoclonal antibodies in human (Davies and Morris 1993). Using these parameters, the AMG 181 concentration–time profiles were simulated under various single SC or IV dosing regimens or multiple SC dosing regimens (Fig. 6). The EC_{50} , EC_{75} , EC_{90} , and EC_{99} values for AMG 181 occupancy of free $\alpha_4\beta_7$ receptors on CD4^+ T cell in humans were assumed to be the same as those estimated in monkeys and are given as reference concentration levels for the

pharmacologic effect in Figure 6A. These levels were used to assess the duration of human AMG 181 concentration over various target saturation levels in designing the subsequent FIH study.

Based on our simulations, the estimated C_{max} at the starting dose of 0.7 mg SC would be associated with approximately 10% of the maximum PD effect (EC_{10}), while the 21, 70, 210, and 420 mg doses were predicted to cover EC_{90} for approximately 2, 3, 5, and 6 months, respectively (Fig. 6A). All four multiple dosing regimens were predicted to maintain AMG 181 concentration above EC_{90} for 3–8 months (Fig. 6B).

The model-predicted AMG 181 C_{max} and AUC values in humans, based on the simulated PK profiles, are presented in Figure 6, and the estimated exposure margins relative to the NOAEL of 80 $\text{mg}\cdot\text{kg}^{-1}$ in cynomolgus

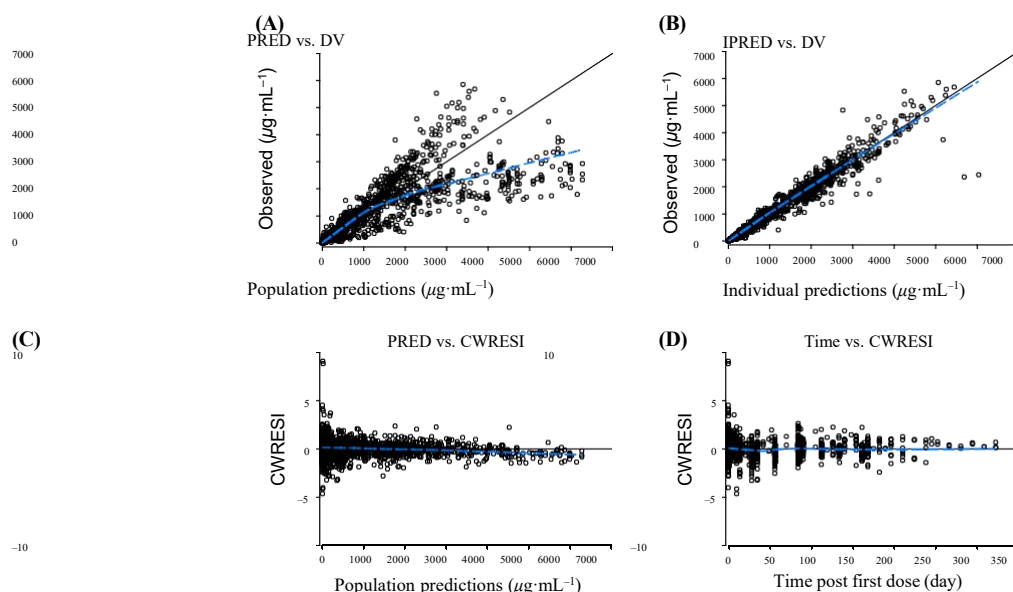


Figure 3. Diagnostic plots for the two-compartment TMDD QE PK model: (A) Observed versus population predicted concentrations. (B) Observed vs. individual Bayesian predicted concentrations. (C) Conditional weighted residuals with interactions versus population predicted concentrations. (D) Conditional weighted residuals with interactions versus time post first dose. Symbols are observations and the blue lines are LOESS regression (local regression) lines. The black lines in (A) and (B) are lines of unity, while, in (C) and (D), lines of zero CWRESI.

Table 2. AMG 181 PK parameter estimates in cynomolgus monkeys through simultaneous fitting of the individual AMG 181 concentration-time data using the two-compartment pharmacokinetic target-mediated drug disposition (TMDD) model with quasi-equilibrium (QE) approximation.

PK parameter (unit)	Estimate (%SE)	IIV (%SE)
K_A (day ⁻¹)	0.846 (3.8)	NE
CL (mL·day ⁻¹)	12.9 (5.9)	44.1 (20)
V_c (mL)	116 (7.9)	46.1 (17)
K_{12} (day ⁻¹)	0.617 (13)	Fixed to 0
K_{21} (day ⁻¹)	0.877 (8.8)	Fixed to 0
K_d (nmol·L ⁻¹)	Fixed to 0.013	Fixed to 0
R_{tot} (nmol·L ⁻¹)	9.18 (20)	180 (23)
K_{int} (day ⁻¹)	0.0215 (6.0)	Fixed to 0
Correlation CL, V_c	0.642 (27)	
Proportional residual error (% CV)	20.1 (1.9)	
Additive residual error SD (nmol·L ⁻¹)	1.11 (14)	

CV, coefficient of variation; IIV, interindividual variability; NE, not estimated.

monkeys are listed in Table 4. Based on these exposure ratios, a greater than 490,000-fold safety margin at the starting dose of 0.7 mg SC in healthy subjects was anticipated. This low starting dose of 0.7 mg was selected because it was predicted to only briefly cover the predicted EC₁₀, in accordance with the Minimal Anticipated Biological Effect Level (MABEL, EMA 2007; Lowe et al.

2010; Yu et al. 2011) guidance by the European Medicines Agency (EMA). Also, based on the US FDA guidance on “Estimating the Maximum Safe Starting Dose in Initial Clinical Trials for Therapeutics in Adult Healthy

Volunteers” (FDA 2005), the starting dose of 0.7 mg was approximately 1/260th of the calculated maximum recommended safe starting dose (MRSD). The MRSD was calculated to be 2.58 mg·kg⁻¹ based on the body surface scaling with exponent 0.67, with an average body weight of 3 kg for monkeys and 60 kg (per MRSD FDA guidance) for humans, a NOAEL of 80 mg·kg⁻¹ in monkeys, and a default safety factor of 10.

Comparison of predicted versus observed AMG 181 PK in humans

The observed AMG 181 C_{max} and AUC_{inf} values in the FIH study were well predicted based on scaling of cynomolgus monkey PK (Fig. 7). With the exception of lower doses (0.7 and 2.1 mg AMG 181), where C_{max} and AUC_{inf} were underpredicted, the observed human AMG 181 C_{max} and AUC_{inf} values were within twofold of the predicted values, consistent with what has previously been reported for allometric scaling of monoclonal antibody PK from cynomolgus monkey to human (Dong et al. 2011). Given the large exposure margins at the proposed FIH starting dose of 0.7 mg, this slight underprediction was not expected to have consequences for patient safety.

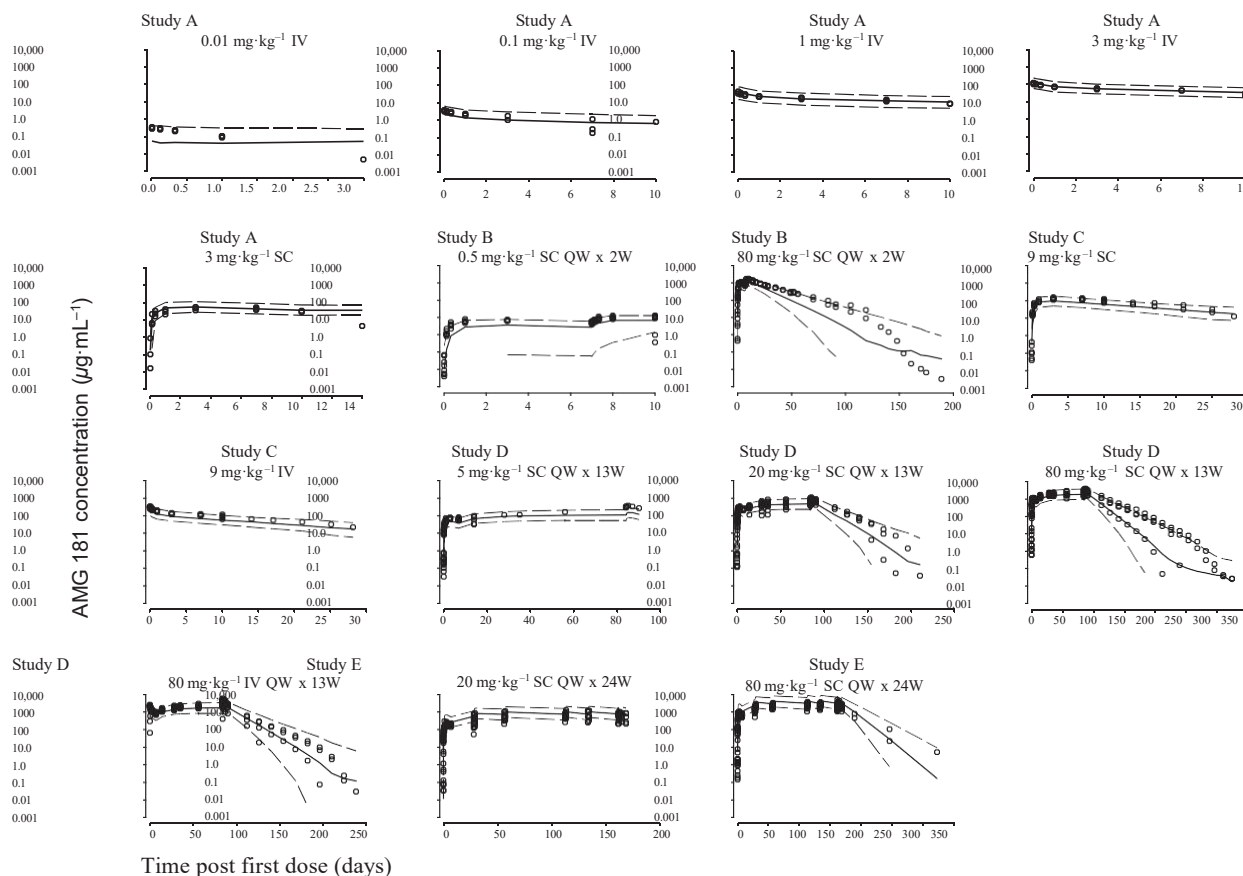


Figure 4. Visual predictive checks for the two-compartment TMDD QE PK model (by cohort): median predictions (solid lines) with 80% confidence intervals (10th and 90th percentiles; dashed lines). Symbols represent observed individual AMG 181 concentrations.

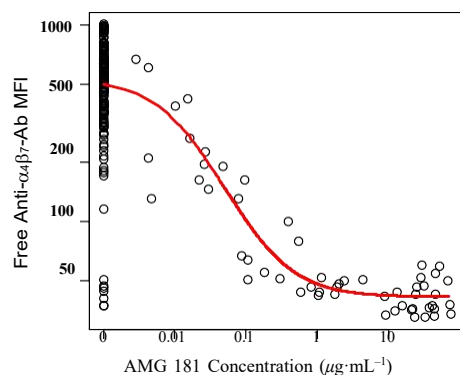


Figure 5. Individual observed free $\alpha_4\beta_7$ receptor on $CD4^+$ T cells (expressed as mean fluorescence intensity (MFI) of the detecting antibody for the free $\alpha_4\beta_7$ receptor) versus AMG 181 concentrations (symbol). The line represents the E_{max} PD model fitting of the observed data.

Discussion and Conclusions

AMG 181 is a human monoclonal antibody that specifically targets intestinal-homing T cells and has been tested

Table 3. Estimated human AMG 181 pharmacokinetic parameters. The PK parameters CL , V_c , K_{12} , and K_{21} were allometric scaled from cynomolgus monkeys. F_1 , K_d , K_{int} , and R_{tot} were assumed to be the same as the cynomolgus monkeys' parameters.

PK parameter (unit)	Human estimate
F_1	1.0 (NS)
K_A (day^{-1})	0.846 (NS)
CL ($\text{mL} \cdot \text{day}^{-1}$)	144
V_c (mL)	2900
K_{12} (day^{-1})	0.276
K_{21} (day^{-1})	0.392
K_d ($\text{nmol} \cdot \text{L}^{-1}$)	0.013 (NS)
R_{tot} ($\text{nmol} \cdot \text{L}^{-1}$)	9.18 (NS)
K_{int} (day^{-1})	0.0215 (NS)

NA, not applicable; NS, not scaled.

for pharmacological activity in vitro as well as for safety and PK/PD in vivo in the pharmacologically relevant species *M. fascicularis* (cynomolgus monkey) (Pan et al. 2014). This report presents a quantitative translational approach for the selection of a safe starting dose and pharmacologically relevant single and multiple dose esca-

© 2014 The Authors. *Pharmacology Research & Perspectives* published by John Wiley & Sons Ltd.

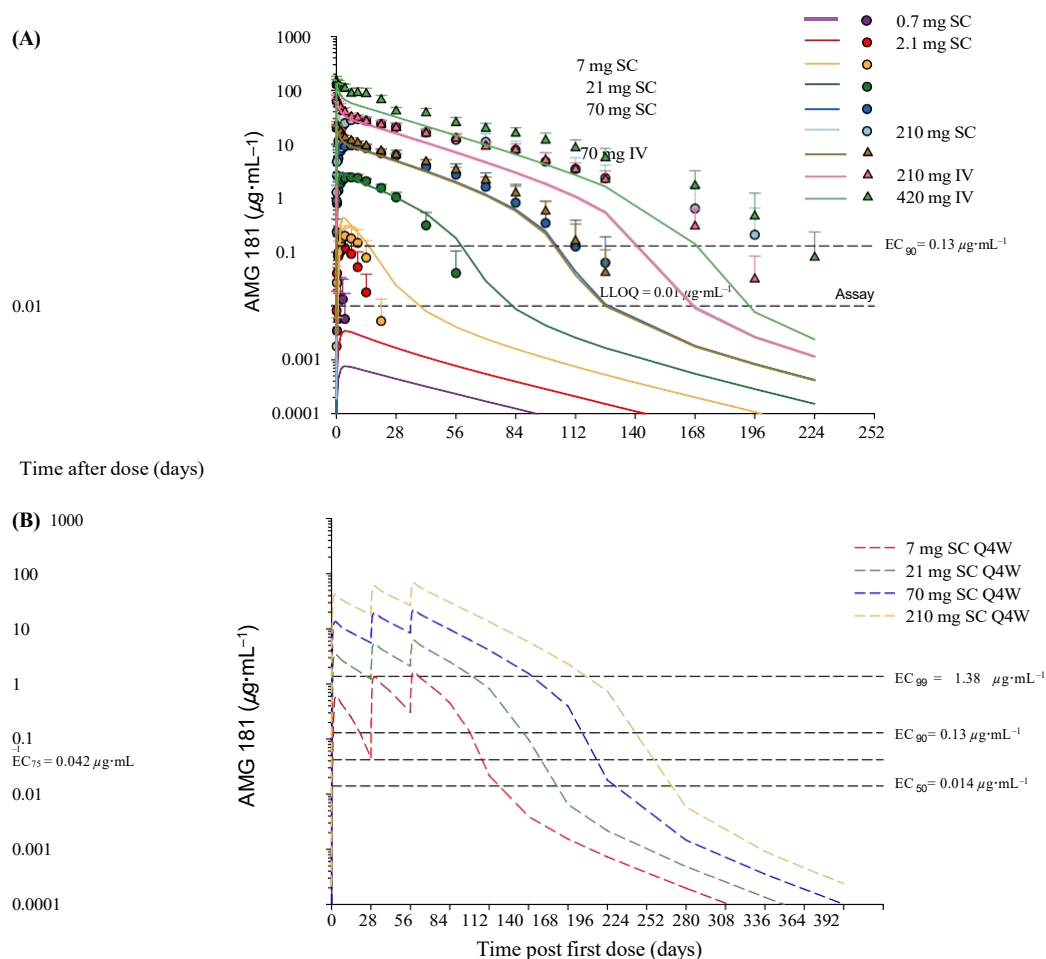


Figure 6. The two-compartment TMDD QE PK model predicted typical AMG 181 PK profiles in humans: (A) Single SC or IV dose (lines) overlaid with the observed mean (SD) data (symbols). (B) Three-monthly SC doses. E_{max} PD model predicted EC_{50} , EC_{75} , EC_{90} , and EC_{99} values are presented to illustrate duration of AMG 181 concentration coverage over a_4b_7 receptor under each dosing regimen.

lation schemes for Phase 1 clinical trials in healthy volunteers and IBD subjects.

Based on visual inspection of the PK profiles in monkeys, AMG 181 disposition was dose- and concentration-dependent with typical linear clearance dominating at higher concentrations and nonlinear clearance dominating at low concentrations ($<1 \text{ g}\cdot\text{mL}^{-1}$, $\sim 7 \text{ nmol/L}$), likely due to saturable binding of AMG 181 to the target T-cell surface a_4b_7 receptors. To describe the parallel linear and nonlinear disposition, a TMDD model (Mager and Jusko 2001) was utilized and all individual monkey AMG 181 concentration–time data were fitted simultaneously.

AMG 181 binds to a_4b_7 receptor with high affinity with a dissociation constant ($K_D = K_{\text{off}}/K_{\text{on}}$) of $13 \text{ pmol}\cdot\text{L}^{-1}$, suggesting that the drug–target association is faster than drug dissociation/distribution/elimination as well as elimination of the target and drug–target complex. In this case, the QSS approximation to TMDD, which assumes

that drug–target complex rapidly approaches a quasi-steady state, is reasonable (Gibiansky and Gibiansky 2009). To overcome the difficulties with model parameter identifiability during model development, QSS model was further simplified to a QE model with $K_{\text{ss}} = K_d = k_{\text{off}}/k_{\text{on}}$.

During the model development, fitting of an empirical two-compartment PK model with parallel linear and nonlinear Michaelis–Menten (M-M) (Dong et al. 2011) elimination was also attempted. The M-M model fit similarly well to the high concentration data as did the TMDD models, but underpredicted concentrations at the terminal elimination phase where AMG 181 concentration were $<0.1 \text{ g}\cdot\text{mL}^{-1}$ (Fig. S3A and B); consistent with what has been demonstrated by Gibiansky and Gibiansky (2009), Yan et al. (2010). The exception to this was for the lowest dose ($0.01 \text{ mg}\cdot\text{kg}^{-1}$ IV) where, unexpectedly, the M-M model provided a better model fit than QE TMDD model.

Table 4. Predicted AMG 181 pharmacokinetic exposure parameters in humans based on the two-compartment model with target-mediated drug disposition (TMDD) and quasi-equilibrium (QE) approximation.

Proposed human dose			PK parameter		Exposure ratio	
Dose (mg)	Dose (mg·kg ⁻¹)	Route	C _{max} (lg·mL ⁻¹)	AUC _{0-inf} or AUC _{tau} (lg·h·mL ⁻¹)	C _{max}	AUC _{0-inf}
Single ascending dose study						
0.7	0.01	SC	0.0009	0.985	5520000	492000
2.1	0.03	SC	0.004	3.81	1120000	127000
7	0.1	SC	0.604	186	8030	2610
21	0.3	SC	3.48	1940	1390	250
70	1	SC	13.5	9500	358	51
210	3	SC	42.4	32,300	114	15
70	1	IV	22.7	9520	214	51
210	3	IV	70.8	32,300	69	15
420	6	IV	143	67,000	34	7
Multiple ascending dose study (Q4W 9 3): after the 3rd dose						
7	0.1	SC	1.69	782	2870	620
21	0.3	SC	6.29	4120	771	118
70	1	SC	22.4	17,100	217	28
210	3	SC	68.4	55,300	71	9

The exposure ratios (margins) were calculated based on NOAEL of 80 mg·kg⁻¹ in cynomolgus monkeys (AUC_{tau}: AUC within the 3rd dosing inter- val for the ascending multiple dose study).

For our purpose, selection of either M-M model or QE TMDD model would have been sufficient to inform selection of FIH dosing. The TMDD QE model was chosen for further analyses and human dose predictions due to better overall model fit at clinically relevant doses.

Three factors posed challenges for better estimation of the AMG 181 PK across all concentrations and dose routes. First, AMG 181 is a human antibody and would unavoidably be immunogenic in monkeys, especially at lower concentrations. Second, only a limited number of monkeys were assigned to the recovery phase of the GLP studies. Both factors reduced the potential amount of PK data available for modeling the terminal elimination phase. Third, the relatively higher exposures observed after SC administration of 80 mg·kg⁻¹ AMG 181 than after IV administration of the same dose (Studies B and D vs. Study D, Fig. 2B) was undoubtedly a challenge for the model to reconcile. While this could potentially be explained by PK variability and small sample sizes, the observed differences could also have stemmed from non-neutralizing AMG 181 immune complex formation, which might have served as a reservoir (Chirmule et al. 2012) for AMG 181 through gradual disassociation and slow release of AMG 181 during the terminal elimination phase. The estimated slow half-life of ~32 days (= 0.693/*K_{int}*) for *a4b7* receptor internalization may support this hypothesis and thus *K_{int}* might be a measure of both target receptor internalization and immune complex elimination.

The immunogenic response against AMG 181 clearly impacted specific PK data points, as illustrated for two

representative animals in Figure S2. For this reason, 120 ADA-positive concentration–time points (representing less than 7% of total data) were excluded from model. This approach is conservative from a safety perspective as it resulted in higher estimated exposures in monkey and consequently in human. Additionally, since AMG 181 is a human IgG2, it is anticipated to carry less immunogenic potential in humans. Indeed, no ADAs were reported in the Ph1a study (Pan et al. 2014).

Dong et al. (2011) suggest that translation of nonlinear elimination to human might be improved by accounting for the between-species difference in target expression and binding. The lack of knowledge of *a4b7* receptor abundance in cynomolgus monkeys and human necessitated the assumption that AMG 181 has the same in vivo pharmacology characteristics and *a4b7* receptor abundance in cynomolgus monkeys and humans. This assumption was justified based on similar in vitro binding to primary T cells and blocking of *a4b7*:MAdCAM-1 binding on primary T cells and T-cell adhesion for cynomolgus monkey and human (Pan et al. 2013). Additionally, potential differences are not expected to affect patient safety due to the large observed safety margins.

The 75% and 90% receptor occupancy levels for natalizumab (anti-*a4*) and vedolizumab (anti-*a4b7*) have been reported to be related to the clinical efficacy in multiple sclerosis (FDA 2003) and IBD (Feagan et al. 2005, 2008). Therefore, the AMG 181 EC₇₅ and EC₉₀ values for *a4b7* receptor occupancy were used as guides to aid the selection of AMG 181 dosing regimens in UC and CD clinical trials: 7, 21, 70, or 210 mg SC once every 1, 2, 3, or

4 months, respectively, would maintain AMG 181 concentration above EC₉₀ within each dosing interval (Fig.

6B) and thus should be efficacious.

Analysis of the available clinical PK, safety and efficacy data from the ongoing studies have shown consistency with our prediction results as shown in Figure 7 (Pan et al. 2014). The predictions of C_{\max} and AUC were within twofold for single doses between 7 and 420 mg which is well accepted for large and small molecules (Hosea et al. 2009; Dong et al. 2011).

In conclusion, AMG 181 in vivo pharmacology from cynomolgus monkeys was successfully translated to humans using the described quantitative translation approach. The developed model was successfully employed to support the selection of a safe starting dose and pharmacologically as well as clinically relevant single and multiple dose escalation schemes for AMG 181 clinical trials in healthy volunteers and IBD subjects.

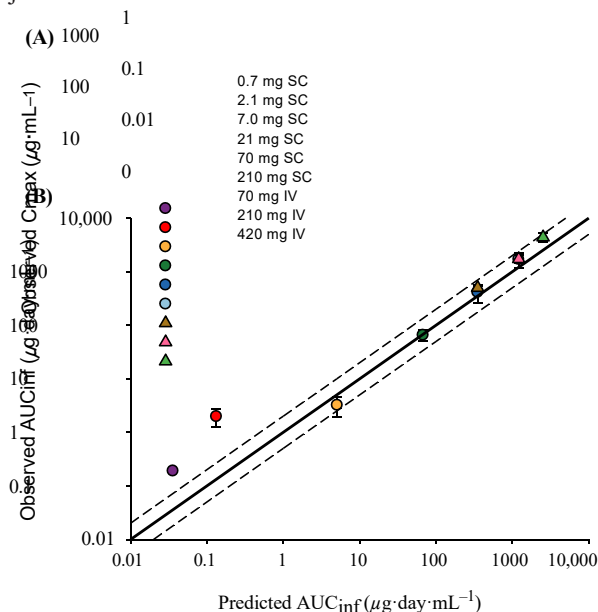


Figure 7. The mean (SD) observed AMG 181 C_{\max} (A) and AUC_{inf} (B) data versus the values calculated using the two-compartment TMDD QE PK model predictions in humans after single SC or IV dose. The middle lines represent the lines of unity, while the upper and lower lines represent the lines of 2-fold of unity.

Chirmule N, Jawa V, Meibohm B (2012). Immunogenicity to therapeutic proteins: impact on PK/PD and efficacy. *AAPS J* 14: 296–302.

Davies B, Morris T (1993). Physiological parameters in laboratory animals and humans. *Pharm Res* 10: 1093–1095.

Dong JQ, Salinger DH, Endres CJ, Gibbs JP, Hsu CP, Stouch BJ, et al. (2011). Quantitative prediction of human pharmacokinetics for monoclonal antibodies: retrospective analysis of monkey as a single species for first-in-human prediction. *Clin Pharmacokinet* 50: 131–142.

EMA (2007). Guideline on requirements for first-in-man clinical trials for potential high-risk medicinal products, Vol. 2012, 3/6/2007 edn. Committee for Medicinal Products for Human Use, http://www.ema.europa.eu/docs/en_GB/document_library/Scientific_guideline/2009/09/WC500002989.pdf.

Disclosures

AMG 181 is being codeveloped by MedImmune, LLC, a wholly owned subsidiary of AstraZeneca plc., and Amgen Inc. and may be referred to as AMG 181 or MEDI7183.

All authors are former or current employees and shareholders or contractors of Amgen Inc.

References

- Apostolaki M, Manoloukos M, Roulis M, Wurbel MA, Muller W, Papadakis KA, et al. (2008). Role of beta7 integrin and the chemokine/chemokine receptor pair CCL25/CCR9 in modeled TNF-dependent Crohn's disease. *Gastroenterology* 134: 2025–2035.
- Beal SS, Boeckmann LB, Bauer RJ (2009). NONMEM user's guides (1989–2009). ICON Development Solutions, Ellicott City, MD.
- Berger JR, Koralnik IJ (2005). Progressive multifocal leukoencephalopathy and natalizumab—unforeseen consequences. *N Engl J Med* 353: 414–416.
- Chen B, Dong JQ, Pan WJ, Ruiz A (2012). Pharmacokinetics/pharmacodynamics model-supported early drug development. *Curr Pharm Biotechnol* 13: 1360–1375.
- FDA (2003). Natalizumab clinical pharmacology and biopharmaceutics review(s). Vol. 2012, US Food and Drug Administration.
- FDA (2005). Estimating the maximum safe starting dose in initial clinical trials for therapeutics in adult healthy volunteers, Vol. 2012, 7/6/2005 edn. US Food and Drug Administration.
- Feagan BG, Greenberg GR, Wild G, Fedorak RN, Pare P, McDonald JW, et al. (2005). Treatment of ulcerative colitis with a humanized antibody to the alpha4beta7 integrin. *N Engl J Med* 352: 2499–2507.
- Feagan BG, Greenberg GR, Wild G, Fedorak RN, Pare P, McDonald JW, et al. (2008). Treatment of active Crohn's disease with MLN0002, a humanized antibody to the alpha4beta7 integrin. *Clin Gastroenterol Hepatol* 6: 1370–1377.
- Fedyk ER, Wyant T, Yang LL, Csizmadia V, Burke K, Yang H, et al. (2012). Exclusive antagonism of the alpha(4) beta(7) integrin by vedolizumab confirms the gut-selectivity of this

pathway in primates. *Inflamm Bowel Dis* 18: 2107–2119.

Gibbs JP (2010). Prediction of exposure-response relationships to support first-in-human study design. *AAPS J* 12: 750–758.

Gibiansky L, Gibiansky E (2009). Target-mediated drug disposition model: approximations, identifiability of model parameters and applications to the population pharmacokinetic-pharmacodynamic modeling of biologics. *Expert Opin Drug Metab Toxicol* 5: 803–812.

Gibiansky L, Gibiansky E, Kakkar T, Ma P (2008). Approximations of the target-mediated drug disposition model and identifiability of model parameters. *J Pharmacokinet Pharmacodyn* 35: 573–591.

Hesterberg PE, Winsor-Hines D, Briskin MJ, Soler-Ferran D, Merrill C, Mackay CR, et al. (1996). Rapid resolution of chronic colitis in the cotton-top tamarin with an antibody to a gut-homing integrin alpha 4 beta 7. *Gastroenterology* 111: 1373–1380. Hosea NA, Collard WT, Cole S, Maurer TS, Fang RX, Jones H, et al. (2009). Prediction of human pharmacokinetics from preclinical information: comparative accuracy of quantitative prediction approaches. *J Clin Pharmacol* 49: 513–533.

Hsu H, Foltz I, Arora T, Jacobsen FW (2010). Alpha-4 beta-7 heterodimer specific (US 2010/0254975 A1). Office USP (ed) Vol. A1. Alexandria, VA, USA.

Hynes RO (2002). Integrins: bidirectional, allosteric signaling machines. *Cell* 110: 673–687.

Lobaton T, Vermeire S, Van Assche G, Rutgeerts P (2014). Review article: anti-adhesion therapies for inflammatory bowel disease. *Aliment Pharmacol Ther* 39: 579–594.

Lowe PJ, Tannenbaum S, Wu K, Lloyd P, Sims J (2010). On setting the first dose in man: quantitating biotherapeutic drug-target binding through pharmacokinetic and pharmacodynamic models. *Basic Clin Pharmacol Toxicol* 106: 195–209.

Polman CH, O'Connor PW, Havrdova E, Hutchinson M, Kappos L, Miller DH, et al. (2006). A randomized, placebo-controlled trial of natalizumab for relapsing multiple sclerosis. *N Engl J Med* 354: 899–910.

Pullen N, Molloy E, Carter D, Syntin P, Clemo F, Finco-Kent D, et al. (2009). Pharmacological characterization of PF-00547659, an anti-human MAdCAM monoclonal antibody. *Br J Pharmacol* 157: 281–293.

Sandborn WJ, Colombel JF, Enns R, Feagan BG, Hanauer SB, Lawrance IC, et al. (2005). Natalizumab induction and maintenance therapy for Crohn's disease. *N Engl J Med* 353: 1912–1925.

Stefanich EG, Danilenko DM, Wang H, O'Byrne S, Erickson R, Gelzleichter T, et al. (2011). A humanized monoclonal antibody targeting the beta7 integrin selectively blocks intestinal homing of T lymphocytes. *Br J Pharmacol* 162: 1855–1870.

Targan SR, Feagan BG, Fedorak RN, Lashner BA, Panaccione R, Present DH, et al. (2007). Natalizumab for the treatment of active Crohn's disease: results of the ENCORE Trial. *Gastroenterology* 132: 1672–1683.

Thomas S, Baumgart DC (2012). Targeting leukocyte migration and adhesion in Crohn's disease and ulcerative colitis. *Inflammopharmacology* 20: 1–18.

Wagner N, Lohler J, Kunkel EJ, Ley K, Leung E, Krissansen G, et al. (1996). Critical role for beta7 integrins in formation of the gut-associated lymphoid

tissue. *Nature* 382: 366–370.

Mager DE, Jusko WJ (2001). General pharmacokinetic model for drugs exhibiting target-mediated drug disposition. *J Pharmacokinet Pharmacodyn* 28: 507–532.

Mager DE, Krzyzanski W (2005). Quasi-equilibrium pharmacokinetic model for drugs exhibiting target-mediated drug disposition. *Pharm Res* 22: 1589–1596.

National Research Council US (2011). Guide for the care and use of laboratory animals. 8th ed. National Academies Press, Washington, DC.

Pan WJ, Lear SP, Patel SK, Prince PJ, Doherty DR, Tam CY, et al. (2012). Pharmacokinetics and pharmacodynamics in cynomolgus monkeys of AMG 181, a fully human anti- $\alpha 4 \beta 7$ antibody for treating inflammatory bowel disease. *J Crohn's Colitis* 6: pS14.

Pan WJ, Hsu H, Rees WA, Lear SP, Lee F, Foltz IN, et al. (2013). Pharmacology of AMG 181, a human anti- $\alpha 4 \beta 7$ antibody that specifically alters trafficking of gut-homing T cells. *Br J Pharmacol* 169: 51–68.

Pan WJ, Kock K, Rees WA, Sullivan BA, Evangelista CM, Yen M, et al. (2014). Clinical pharmacology of AMG 181, a gut-specific human anti- $\alpha 4 \beta 7$ monoclonal antibody, for treating inflammatory bowel diseases. *Br J Clin Pharmacol* Epub ahead of print.

Parikh A, Leach T, Wyant T, Scholz C, Sankoh S, Mould DR, et al. (2011). Vedolizumab for the treatment of active ulcerative colitis: a randomized controlled phase 2 dose-ranging study. *Inflamm Bowel Dis* 18: 1470–1479.

Picarella D, Hurlbut P, Rottman J, Shi X, Butcher E, Ringler DJ (1997). Monoclonal antibodies specific for beta 7 integrin and mucosal addressin cell adhesion molecule-1 (MAdCAM-1) reduce inflammation in the colon of scid mice reconstituted with CD45RBhigh CD4+ T cells. *J Immunol* 158: 2099–2106.

tissue. *Nature* 382: 366–370.

Yan X, Mager DE, Krzyzanski W (2010). Selection between Michaelis-Menten and target-mediated drug disposition pharmacokinetic models. *J Pharmacokinet Pharmacodyn* 37: 25–47.

Yu J, Karcher H, Feire AL, Lowe PJ (2011). From target selection to the minimum acceptable biological effect level for human study: use of mechanism-based PK/PD modeling to design safe and efficacious biologics. AAPS J 13: 169–178.

Zou P, Yu Y, Zheng N, Yang Y, Paholak HJ, Yu LX, et al. (2012). Applications of human pharmacokinetic prediction in first-in-human dose estimation. AAPS J 14: 262–281.